Bulletin of Geophysics and Oceanography Vol. 67, n. 2, pp. 229-244; June 2026
DOI 10.4430/bgo00500

Palaeoseismic evidence of a mainshock in the Lamezia Terme area during the March 1638 seismic sequence (M_W ~7, Calabria, southern Italy)

P. Galli[1,2], F. Muto[3] and E. Peronace[2]

[1] *Dipartimento Protezione Civile, Rome, Italy*
[2] *IGAG, Consiglio Nazionale delle Ricerche, Rome, Italy*
[3] *DiBEST, Università delle Calabria, Cosenza, Italy*

(Received: 10 June 2025; accepted: 2 August 2025; published online: 18 September 2025)

ABSTRACT Among the devastating earthquakes to have struck the Italian peninsula are those of the March-June 1638 sequence in central Calabria, which caused over 10,000 deaths and an unprecedented level of destruction spanning from the Tyrrhenian to the Ionian seas. Currently, Italian seismic catalogues report the macroseismic epicentres of two mainshocks: one on 27 March located on the south-western slopes of the Sila plateau (M_W 7.1), and another on 8 June on the eastern side of the Sila (M_W 6.8). However, neither of these epicentres fully explains the complex distribution of the highest intensities. Palaeoseismological studies conducted in the 2000s identified the source of the June earthquake in the inner Sila plateau (Lakes Fault). Meanwhile, historical investigations suggested that two mainshocks occurred in March: one on Saturday 27, between the upper Crati and Savuto river valleys, and another on Sunday 28, in the western Catanzaro Strait. New palaeoseismological evidence, together with indications of active tectonics, supports the hypothesis that the mainshock on 28 March was generated by the rupture of the northern border fault of the Sant'Eufemia plain (Sant'Eufemia Fault). This normal fault likely extends westwards well beyond the Tyrrhenian coastline into the Gulf of Sant'Eufemia, with a WSW–ENE trend.

Key words: Late Pleistocene tectonics, palaeoseismology, historical seismology, 1638 Calabrian earthquakes, Sant'Eufemia Fault.

1. Introduction

The Calabrian seismic sequence of March-June 1638 ranks among the most destructive in the history of southern Italy, involving multiple mainshocks originating from distinct and distant faults (Galli, 2024). Earthquakes caused widespread devastation across central Calabria, from the Tyrrhenian to the Ionian seas, and resulted in at least 10,000 casualties. In different Italian seismic catalogues (e.g. Postpischl, 1985; Camassi and Stucchi, 1997; Guidoboni *et al*., 2018; Rovida *et al*., 2022), the sequence is parametrised with a mainshock on 27 March (M_W estimated between 6.1 and 7.3, according to the different catalogues), followed by another mainshock on 8 June (M_W between 5.6 and 6.9; epicentres are shown as white stars 1 and 2 in Fig. 1). A different interpretation is proposed in Galli and Bosi (2003), where the sequence began on 27 March with an M_W ~6.8 mainshock affecting the southern Crati and northern Savuto river valleys. This was followed by a second mainshock on 28 March (M_W ~6.6) in the western Catanzaro Strait (the

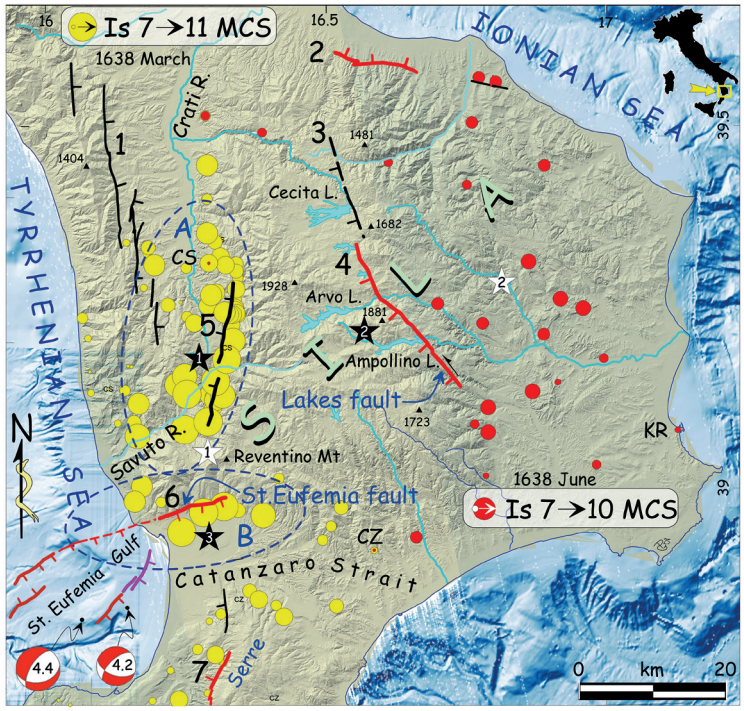

Fig. 1 - Main seismogenic faults of central Calabria (1 = Crati; 2 = Rossano; 3 = Cecita; 4 = Lakes; 5 = Piano Lago-Savuto; 6 = Sant'Eufemia; 7 = Serre North). Red faults have been shown to offset Holocene deposits (Galli and Bosi, 2003; Galli *et al*., 2007, 2010). Offshore red-brick faults displace the seafloor by > 20 m; magenta faults are buried after the last glacial maximum unconformity (Martorelli *et al*., 2023). Tick marks on hanging-wall. Yellow circles, 27–28 March Mercalli-Cancani-Sieberg (MCS) intensity data points (8 ≤ *Is* ≤ 11); red circles, June 1638 MCS intensity data points (8 ≤ *Is* ≤ 10). Blue ellipses, mesoseismic area of the 1638, 27 March (A) and 28 March (B), earthquakes (modified after Galli and Bosi, 2003). White stars 1-2, epicentres of the March and June events according to Rovida *et al*. (2022); black stars 1 to 3 according to Galli and Bosi (2003). CS = Cosenza; KR = Crotone; CZ = Catanzaro.

Sant'Eufemia region, now also named Lamezia Terme area), and a third on 8 June (M_w ~6.7) in central Sila (epicentres are black stars 1 to 3 in Fig. 1).

To date, only the seismogenic source of the June mainshock has been conclusively identified and parametrised, based on data from five palaeoseismic trenches excavated along the previously unknown Lakes Fault (4 in Fig. 1), located in the inner Sila highland (Galli and Bosi, 2003). In contrast, the faults responsible for the March events remain undefined [e.g. Piano Lago-Savuto valley-Decollatura fault system, according to Moretti (2000); 5 in Fig. 1]. To address part of this gap, we have collected new geological, geophysical and geochronological (^{14}C) data along the ENE-WSW striking the Sant'Eufemia Fault (6 in Fig. 1), located within the southernmost part of the March 1638 mesoseismic region, specifically, the area affected by the 28 March event. These findings shed light on the 1638 Calabrian seismic sequence, enhance our understanding of the fault's geometry and behaviour, and offer new insights into its seismogenic potential.

2. Geological framework

The investigated region is part of the Calabrian Arc (CA), which is an arc-shaped orogenic belt primarily composed of exotic metamorphic and intrusive units (Bonardi *et al*., 2001),

wedged between the Southern Apennine Chain and the Maghrebides fold-and-thrust belts (Amodio-Morelli *et al*., 1976). The CA is predominantly made up of Hercynian basement rocks, tectonically emplaced over ophiolite-bearing units of Tethyan affinity (Piluso *et al*., 2000; Alvarez, 2005; Ortolano *et al.*, 2020), which in turn rest upon Mesozoic carbonate platform limestones of Apennine affinity (Ogniben, 1969; Amodio-Morelli *et al*., 1976; Tortorici, 1982; Brandt and Shenk, 2020). The Neogene opening of the western Tyrrhenian Sea was accompanied by intense thrusting within the southern Apennines, related to the progressive eastward migration of the CA over the subducting Ionian lithosphere (Malinverno and Ryan, 1986; Faccenna *et al*., 2005; Critelli *et al*., 2013). This rapid migration led to fragmentation of the CA into structural highs and sedimentary basins (Ghisetti, 1979). As a result, a series of rifting-related, transtensional and extensional basins developed along the inner margin of the orogen during the Upper Miocene–Pleistocene (Van Dijk *et al*., 2000; Muto and Perri, 2002). These include longitudinally oriented structural highs (e.g. the Aspromonte–Sila mountains) and Tyrrhenian basins (e.g. the Crati, Mesima, Gioia Tauro, and Messina Strait basins), interrupted by transverse basins (e.g. the Sibari, Siderno, and Catanzaro troughs) (Ghisetti and Vezzani, 1982).

The Catanzaro Trough is one of the narrow, transversal basins connecting the Ionian and Tyrrhenian seas. It is filled with Neogene–Quaternary deposits that unconformably overlie a Palaeozoic-Mesozoic metamorphic rocks overthrust on the Mesozoic carbonate unit, the latter traditionally interpreted as a tectonic window in the literature [i.e. Caronte tectonic window; Amodio-Morelli *et al*. (1976)]. The basal sedimentary sequence comprises Middle Miocene continental conglomerates, fan-delta deposits, and marine clays, overlain by Messinian limestone and gypsum (Muto *et al*., 2014; Brutto *et al*., 2016). This is followed by Pliocene conglomerates and marls, comparable to the Trubi Formation (Cavazza and DeCelles, 1998), as well as tidalite-bearing sands and sandstones (Longhitano *et al*., 2014; Chiarella *et al*., 2016). The Middle-Upper Pleistocene succession includes conglomerates and sands shaped by both tectonic activity and, especially, glacio-eustatic sea-level fluctuations (Brutto *et al*., 2018). The northern mountain front of the basin is characterised by Upper Pleistocene-Holocene deposits of conglomerates and sands, associated with multiple generations of alluvial fans (Antronico *et al*., 2001; Ruello *et al*., 2017; Russo Ermolli *et al*., 2018).

The structural framework of the Catanzaro Trough is characterised by a WNW–ESE to WSW–ENE trending, left-lateral shear zone (Van Dijk *et al*., 2000). Along the northern margin, the most prominent structure is the Lamezia–Catanzaro fault system, composed of south-dipping, right-stepping *en-echelon* segments (Tansi *et al*., 2007; Brutto *et al*., 2018; Lavecchia *et al*., 2024; see white dashed lines in Fig. 2). During the Late Miocene, this fault system exhibited left-lateral kinematics, which shifted to right-lateral motion during the Piacenzian to Early Pleistocene (Brutto *et al*., 2016). In the western offshore area (Sant'Eufemia Gulf), the WSW–ENE system likely offset the Pliocene-Quaternary basin infill (Fig. 1), with some faults even affecting the seafloor morphology (Loreto *et al*., 2013, 2023; Brutto *et al*., 2016; Corradino *et al*., 2021; Martorelli *et al*., 2023).

3. Historical seismicity

Archive research (Scionti and Galli, 2005; Scionti *et al*., 2006) indicates that the seismic activity in the Catanzaro Strait abruptly started and intensified at the beginning of the 17th century, following a series of scattered events with M_w < 6 occurring in 1609, 1624, and 1626, which preceded the major 1638 earthquakes. Notably, the 20 July 1609 event (M_w 5.8) struck

towns such as Feroleto and Nicastro, both of which were later devastated by the 1638 sequence. This has led to the suggestion that the 1609 earthquake may have been an early foreshock of the 1638 event, potentially involving part of the same seismogenic structure (Scionti and Galli, 2005; Scionti *et al*., 2006). Regarding the 1638 sequence itself, current Italian seismic catalogues (e.g. Guidoboni *et al.*, 2018; Rovida *et al*., 2022) report the macroseismically-derived epicentres of the 27 March and 8 June mainshocks, but omit the numerous foreshocks and aftershocks documented in historical sources. Based on the distribution of the highest Mercalli-Cancani-Sieberg (MCS) scale (Sieberg, 1930), the 27 March epicentre has been located on the south-western slopes of the Sila plateau (Mt. Reventino area; white star 1 in Fig. 1), and the earthquake assigned one of the highest magnitudes ever attributed to an Italian earthquake (M_w 7.1). In contrast, the June event is located along the eastern edge of the Sila plateau (white star 2 in Fig. 1), with an estimated magnitude of M_w 6.8.

However, neither epicentre adequately accounts for the widespread and complex pattern of observed damage [in Fig. 1 see yellow and red macroseismic intensity data points, from Galli and Bosi (2003)], particularly given the mountainous nature of the region, which in the 17th century hosted only sparse settlements within the Sila highland. The existence of this kind of seismological bias was confirmed by palaeoseismological investigations first conducted by Galli and Bosi (2003), and then refined by Galli and Scionti (2006) and Galli *et al*. (2007), who attributed the June mainshock to a newly discovered fault located in the inner Sila plateau, at an elevation of 1300-1500 m a.s.l. (Lakes Fault, 4 in Fig. 1). Notably, the hanging-wall of this fault is over 20 km from the macroseismically inferred epicentre (see black versus white star 2 in Fig. 1).

Regarding the March sequence, Galli and Bosi (2003), drawing on firsthand accounts from distinguished and authoritative eyewitnesses, hypothesise the occurrence of two mainshocks on 27 and 28 March. The first struck the upper Crati and Savuto valleys, while the second impacted the western Catanzaro Strait (see mesoseismic areas in ellipses A-B, plus black star epicentres 1 and 3 in Fig. 1). This latter event occurred in the early afternoon of Sunday 28 and devastated the ancient towns of Falerna, Gizzeria, Castiglione, Sant'Eufemia, Sambiase, Nicastro, and Feroleto (from west to east, see the six largest intensity data points within ellipse B), all of which suffered damage reaching intensity levels from 10 to 11 on the MCS scale. Notably, the renowned Jesuit scholar and scientist Athanasius Kircher, who was travelling from Sicily to Naples at the time, provided a vivid and precise description of the earthquake sequence in his encyclopaedic and naturalistic work "Mundus Subterraneus" (Kircher, 1665). While in Tropea, he recounts how the terrifying series of shocks began on Palm Saturday (27 March), and continued throughout the night. On Palm Sunday (28 March), as he approached the village of Sant'Eufemia Vetere and its magnificent 11th-century Norman abbey, he wrote: *"The place on which we stood now began to shake most dreadfully: so that being unable to stand, my companions and I caught hold of whatever shrub grew next to us, and supported ourselves in that manner. After some time, this violent paroxysm ceasing, we again stood up, in order to prosecute our voyage to Euphaemia, which lay within sight* (authors' note: the Monastery of Saint Mary of Sant'Eufemia, founded by the Normans in the 11th century, and the now-vanished city likely located at the site of present-day Sant'Eufemia Vetere)*. In the meantime, while we were preparing for this purpose, I turned my eyes toward the city, but could see only a frightful dark cloud, that seemed to rest upon the place. This the more surprised us, as the weather was so very serene. We waited, therefore, till the cloud had passed away: then turning to look for the city, it was totally sunk. Wonderful to tell! Nothing but a dismal and putrid lake was seen where it stood. We looked about to find someone who could tell us of its sad catastrophe, but could see no person. All was become a melancholy solitude; a scene of hideous desolation.*"

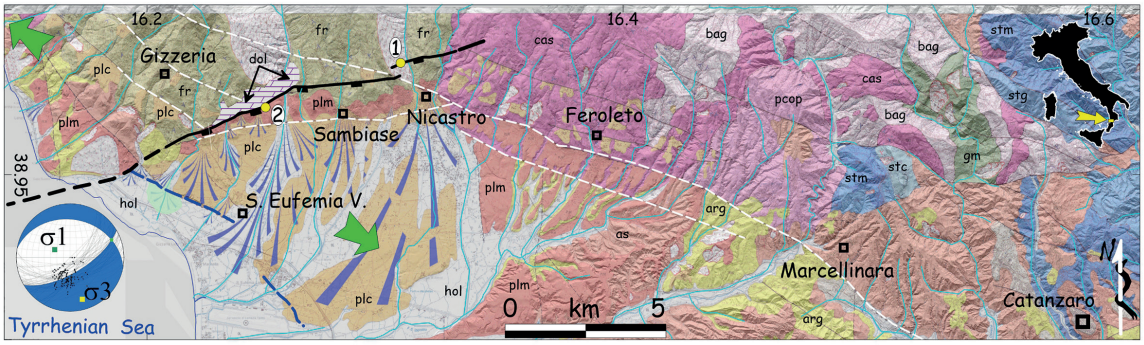

Fig. 2 - Geology of the western Catanzaro Strait (after Antronico *et al.*, 2001): hol = Holocene alluvial-coastal plains; plc/plm = Pleistocene continental/marine terrace; arg/as = Tortonian-Pliocene clay/sand; fr = Frido Unit (argillite schists, phyllites and quartzites); gm = Gimigliano unit (serpentinites, metabasites, and Tithonian-Neocomian cover); bag = Bagni unit (phyllites with metarenites); pcop = Polia-Copanello unit (kinzigitic gneiss); cas = Castagna unit (augen gneiss, paragneiss, micaschists); stg = Stilo unit (granites and granodiorite basement); stm = Stilo unit (phyllites, metacarbonates, paragneiss); dol = Triassic carbonate Apennine chain unit (dolomite, dolomitic limestone). Blue dashed line = Late Pleistocene coastline; white dashed lines = inferred path of the Lamezia-Catanzaro fault system *auctorum*; black line = Sant'Eufemia normal fault (tick marks on hanging-wall; dashed where inferred; see Fig. 1 for possible offshore prolongation); yellow points 1-2 = palaeoseismological sites; blue focal mechanism = pseudo-fault-plane solution from slickenlines (T axis 163°); green arrows = regional extension from Global Navigation Satellite System (GNSS) data (Palano *et al*., 2023).

4. Material and methods

4.1. Field investigations

Field investigations were carried out along the south western hillslope of the Sila plateau, in the area crossed by the Sant'Eufemia Fault, and within its hanging-wall in the facing Sant'Eufemia plain. Geological and structural survey were integrated with field geomorphological observations and 1950s aerial stereopair-photo analyses (NATO photographs, 1:33,000 scale), together with a five-metre digital terrain model (DTM Regione Calabria) implemented with a one-metre-resolution LiDAR survey available on-line (https://gn.mase.gov.it/portale/home).

4.2. Structural analyses

The structural survey was mainly carried out along the Triassic carbonate slickensides. We collected approximately 70 pieces of data related to the hierarchically latest slickenlines visible over the slickenside. For each datum, we measured the slickenside and the slip vector indicated by steps, calcite shear fibre, corrugation, and crescentic markings. The structural data were processed using the FaultKin 8.3.2 software (Allmendinger *et al.*, 2012). By placing the internal friction angle between the fault plane and the P axis θ = 30 °, the T axis and the P axis were calculated for each data (Anderson *et al.*, 1951). By applying the Right Dihedra Method (Angelier and Mechler, 1977) we derived a synthetic pseudo-focal mechanism. We applied FaultKin software for calculating the local stress tensor through the inversion of the fault and stria data. In doing this, we assumed that the slip on the fault planes occurred in the direction of the resolved shear stress, and that the measured data reflect a stress field that is uniform both spatially and temporally [see details in Angelier (1990)].

4.3. Palaeoseismic analyses

Two hand-made diggings were carried out using shovels, pickaxes, and hoes to trim the excavations previously performed by a mechanical excavator. Successively, the exposed walls were scraped, flattened, and equipped with a 0.5- to one-metre-spaced grid and, then, plotted at a 1:20 scale on millimetre graph paper. Hundreds of georeferenced photos were taken with different natural and artificial light and, then, mosaiced and overlaid on the final trench-plot. Samples of organic sediment (palaeosols and colluvia) and charred material were also collected for dating the different stratigraphical units.

4.4. Dating

The age of the deposits has been constrained by radiocarbon analyses (see Table 1). These were performed on bulk samples using the Accelerator Mass Spectrometry (AMS) technique at the Beta Analytic laboratories (Miami, USA). Standards and analytical protocols are available at http://www.radiocarbon.com/.

4.5. Electrical resistivity tomography

Subsurface architecture exploration of the fault zone across the Sant'Eufemia Fault has been attained by means of an IRIS SYSCAL PRO multielectrode and multichannel georesistivimeter with 10 true differential input channels. We used different array configurations (pole-dipole, dipole-dipole, and Wenner-Schlumberger) covering investigation depths in the range of 10-100 m. Data elaboration was performed using ZoneRes2d 7 software produced by Zone-Geophysics (see further details at http://zond-geo.com/english/zond-software/ert-and-ves/zondres2d/).

5. Evidence of active tectonics along the Sant'Eufemia Fault

Although Galli and Bosi (2003) were aware that the geological evidence was rather weak, they tentatively attributed the 28 March 1638 earthquake to a possible activity of the Feroleto–Sant'Eufemia normal/right-lateral fault system [white-dashed line in Fig. 2, western part of the Lamezia-Catanzaro fault system *auctorum*, see Ghisetti (1979), Sorriso-Valvo and Tansi (1996), Moretti (2000), and Antronico *et al*. (2001)]. Subsequently, several other authors claimed for the activity of this fault system, mainly on the basis of: 1) ambiguous and non-decisive geomorphological indicators [e.g. triangular facets (Tansi *et al*., 2007; Brutto *et al*., 2016; Pirrotta *et al*., 2021, 2022)]; 2) presumed fault scarps affecting undated alluvial fan deposits (Tortorici *et al*., 2002; Ruello *et al*., 2017) and/or flights of marine and continental terraces (Brutto *et al*., 2016; Pirrotta *et al*., 2021); 3) subsurface geophysical indications (Punzo *et al*., 2021). Actually, the thick vegetation cover, associated with widespread landsliding and anthropogenic alterations of the hillslopes potentially affected by the faults, has so far prevented the discovery of punctual, conclusive field evidence of surface faulting, making it impossible to confirm fault activity during Holocene and historical times.

Based on 1954 stereoscopic aerial photographs, LiDAR-derived terrain model, and field surveys, we mapped the imprint of a ~N60°-70° striking normal fault (black line in Fig. 2) roughly paralleling one of the fault splays reported in Antronico *et al*. (2001). This fault traverses the hillslopes north of Nicastro and Sambiase, cutting across the flanks of densely forested valleys

incised both into the metamorphic/carbonate basement and the staircase of continental and marine terraces facing the Sant'Eufemia plain. In general, the fault exhibits minimal morphological expression and only a few elusive outcrops, except where it crosses the Mesozoic carbonates exposed within the Caronte tectonic window (dol in Fig. 2). In this sector, it forms a typical rock-fault scarp, marked at its base by a faintly continuous carbonate slickenside (Fig. 3), made by several *en-echelon* segments, with left steps less than a hundred metres wide.

Interestingly, within the Caronte tectonic window, the inner edge of a Middle Pleistocene (?) marine terrace (plm in Fig. 2) is suspended along a rectified limestone hillslope (Fig. 3A), where it abuts a palaeo-cliff carved into an earlier rock-fault scarp. As the marine sands blanket and pervasively fill the fractures within the carbonate slickenside, mantling the rock fault scarp, the

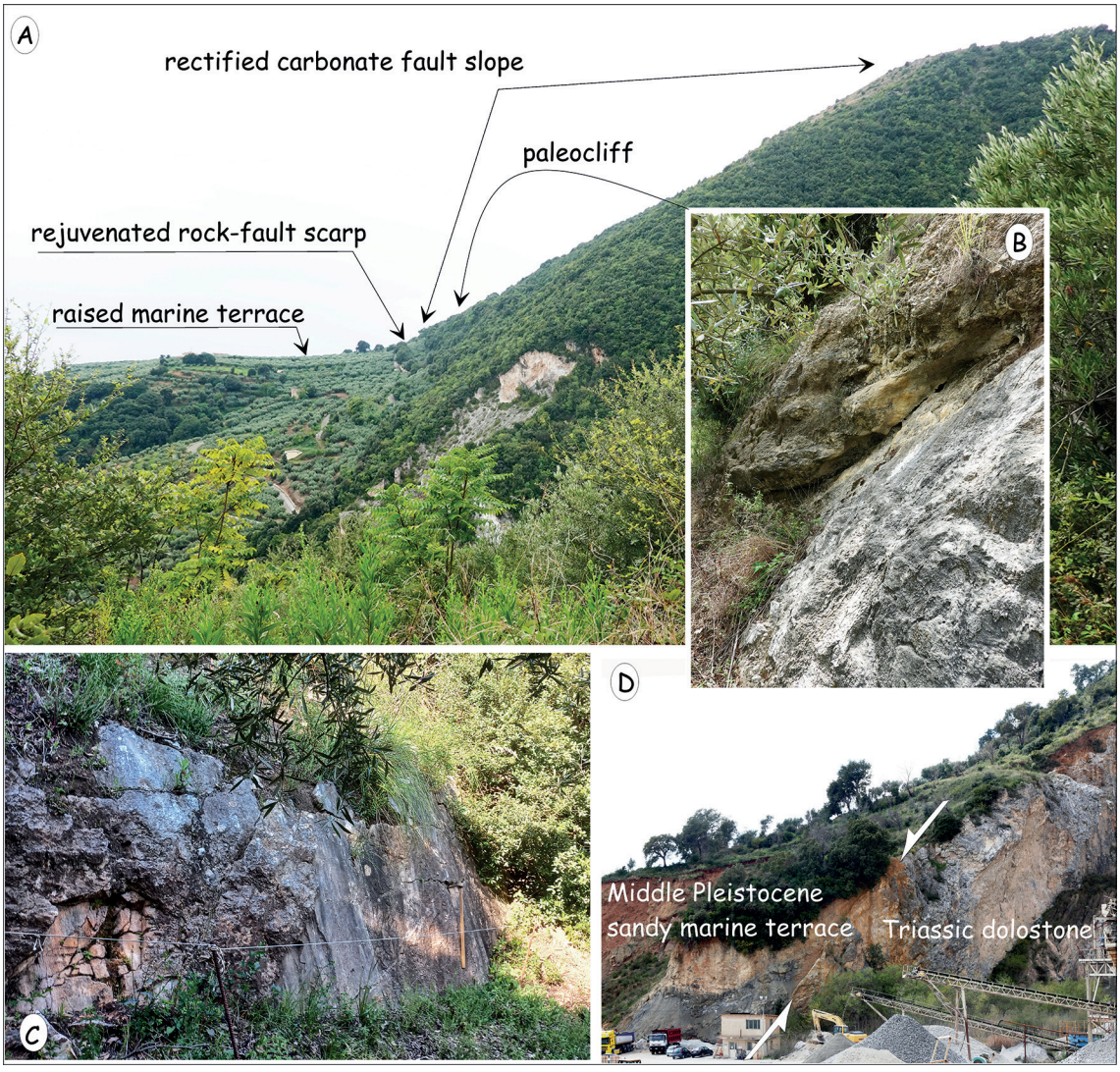

Fig. 3 - A) Westward view of the fault-controlled hillslope developed in the Triassic dolostone (footwall of the Sant'Eufemia Fault); B) close-up of the inner edge of a Middle Pleistocene (?) marine terrace resting against a bedrock cliff carved into the pre-existing rock-fault scarp. The fault successively reactivated, forming a new rock-fault scarp further downslope (C), which discontinuously crops out all along the carbonate Caronte tectonic-window (D).

marine terrace effectively seals the fault itself (Fig. 3B). In contrast, the terrace is clearly displaced by the rejuvenated basal splay of the fault, whose slickenside is exposed several dozen metres downslope (Figs. 3C and 3D), where it can be followed into the thick forest, both westwards and eastwards.

Despite the challenges in identifying unequivocal evidence of fault activity, we report, for the first time, recent surface faulting evidence at two distant sites along the Sant'Eufemia Fault: one within the metamorphic basement of the Frido unit (Vasta site), and the other within the Caronte tectonic window (Scalfaro site), where Triassic dolostones are exposed (sites 1 and 2 in Fig. 2, respectively).

5.1. Vasta site

In this outcrop (1 in Fig. 2), we uncovered a sharp tectonic contact between metamorphic rocks and recent slope debris (Fig. 4) along a N60° striking, 70° dipping plane. The continuity at depth of these two lithologies and the subvertical geometry of their lateral contact has also been highlighted by two electrical resistivity tomographies performed in the forest above the outcrop (e.g. in Fig. 4A).

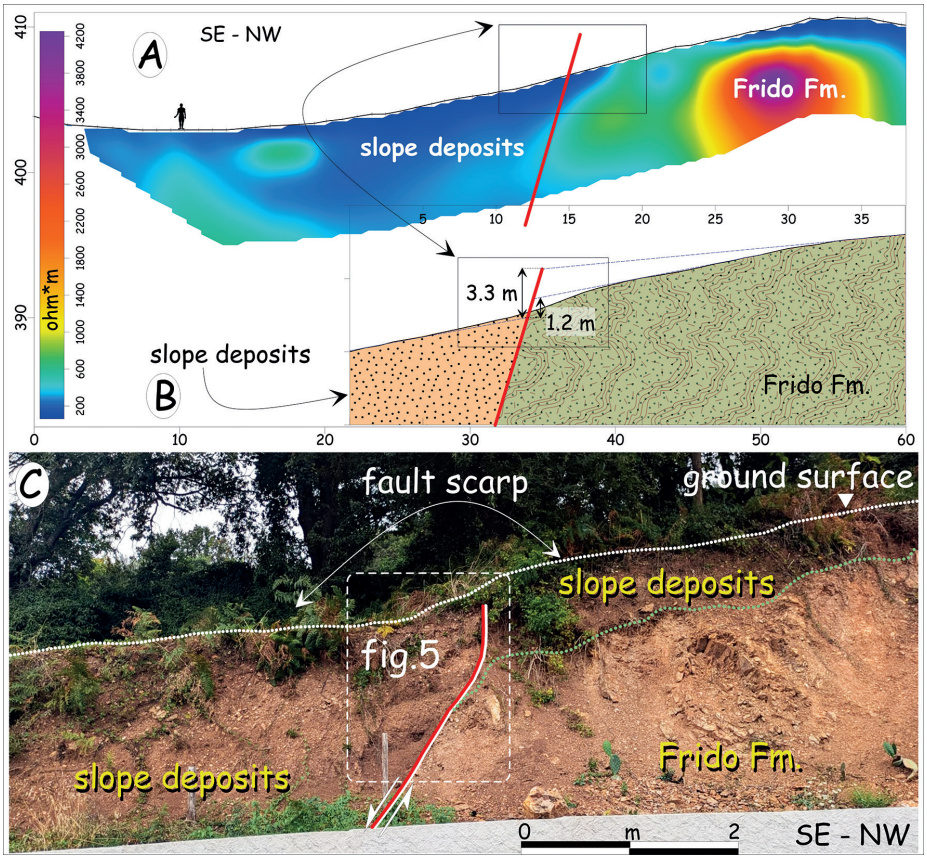

Fig. 4 - A) Electrical resistivity tomography across the fault trace, showing the high resistivity metapelites and quartzites of the Frido metamorphic unit, faulted against the low resistivity slope deposits; B) detailed topographic profile across the composite fault scarp, showing the possible presence of two or more surface faulting events; C) panoramic view of the fault zone (detail in Fig. 5).

Slope deposits (Fig. 4) consist of alternating loose gravels and sandy colluvia (units 3 to 8 in Fig. 5), all of which are faulted and dragged against highly tectonised metapelites and quartzites (Frido Formation *auctorum*, Cretaceous; unit 9). We sampled different layers of the slope deposits obtaining four AMS ages (Table 1), all falling within the second half of the 1st millennium A.D. In the footwall, we were not confident enough to date unit 8 due to its proximity to the ground surface, which could allow contamination by younger organic material. At the upper part of the outcrop, a wedge-shaped gravel unit (4) is buried by a downward-tapering colluvium (3), suggesting a surface faulting event that created a ground step that enabled the deposition of the colluvial wedge (CW). This surface faulting occurred during the pedogenesis of unit 5, a sandy colluvium forming the ground surface at the time of the earthquake. Therefore, the date of the resulting earthquake is around 655-775 A.D. and 605-685 A.D. (rough ages of unit 5 and 4, respectively), and before 895-1025 A.D. (age of unit 3). A subsequent faulting event displaced the entire slope sequence, which is now sealed only by units 1 and 2. This last earthquake occurred significantly after 895-1025 A.D. and, together with the previous one, contributed to forming the compound, retreated fault scarps (e.g. in Galli *et al.*, 2014) currently visible at the top of this outcrop (Fig. 4B).

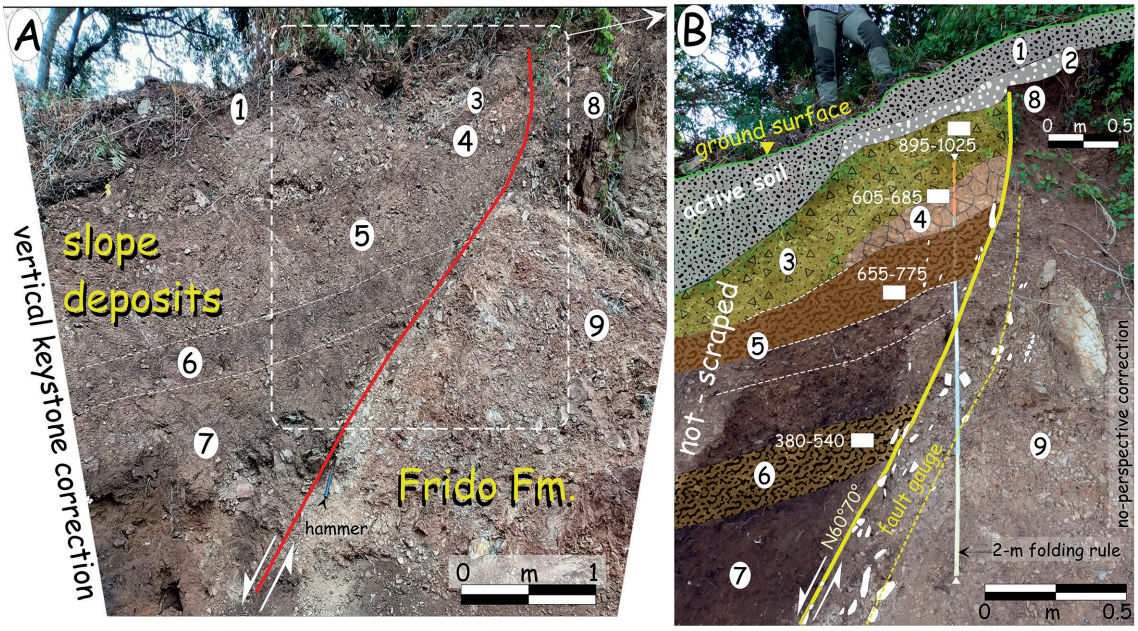

Fig. 5 - A) Close-up view of the outcrop showing the faulting of historical slope deposits against tectonised phyllites and quartzites of the Frido Formation; B) palaeoseismic sketch of the fault zone. AMS dating of four samples (A.D. ages) suggests a first surface faulting event around 700 A.D., followed by a more recent within the past millennium, likely associated with the 28 March 1638 earthquake.

5.2. Scalfaro site

By following the approximately 3-kilometre-long slickenside outcrops carved into the dolostone within the Caronte tectonic window, we identified evidence of surface faulting on the left side of a deeply incised, ~N-S-trending stream that intersects the fault zone nearly perpendicularly (2 in Fig. 2). The stream has cut its bed into the Triassic dolostone of the Caronte tectonic window and into remnants of a marine terrace faulted against the dolostone (Fig. 6A),

Table 1 - ^{14}C age of organic material sampled in trenches or pits along the Sant'Eufemia fault system.

Site	Sample	Laboratory	Analysis	Dated material	$\delta^{13}C$ (o/oo)	Conventional age (B.P.)	2σ cal. 95%
Vasta	LCZ01	Beta-703292	AMS	Organic sediment	-25.60	1070±30	895-1025 A.D.
	LCZ02	Beta-703293	AMS	Organic sediment	-25.40	1320±30	655-775 A.D.
	LCZ03	Beta-703294	AMS	Organic sediment	-26.10	1370±30	605-685 A.D.
	LCZPS-05	Beta-720314	AMS	Organic sediment	-26.00	1630±30	380-540 A.D.
Scalfaro	SCLFR01	Beta-747192	AMS	Organic sediment	-25.27	101.13±0.38 pMC	1955-2019 A.D.
	SCLFR02	Beta-747193	AMS	Organic sediment	-24.75	5120±0.30	5830-5854 B.P.

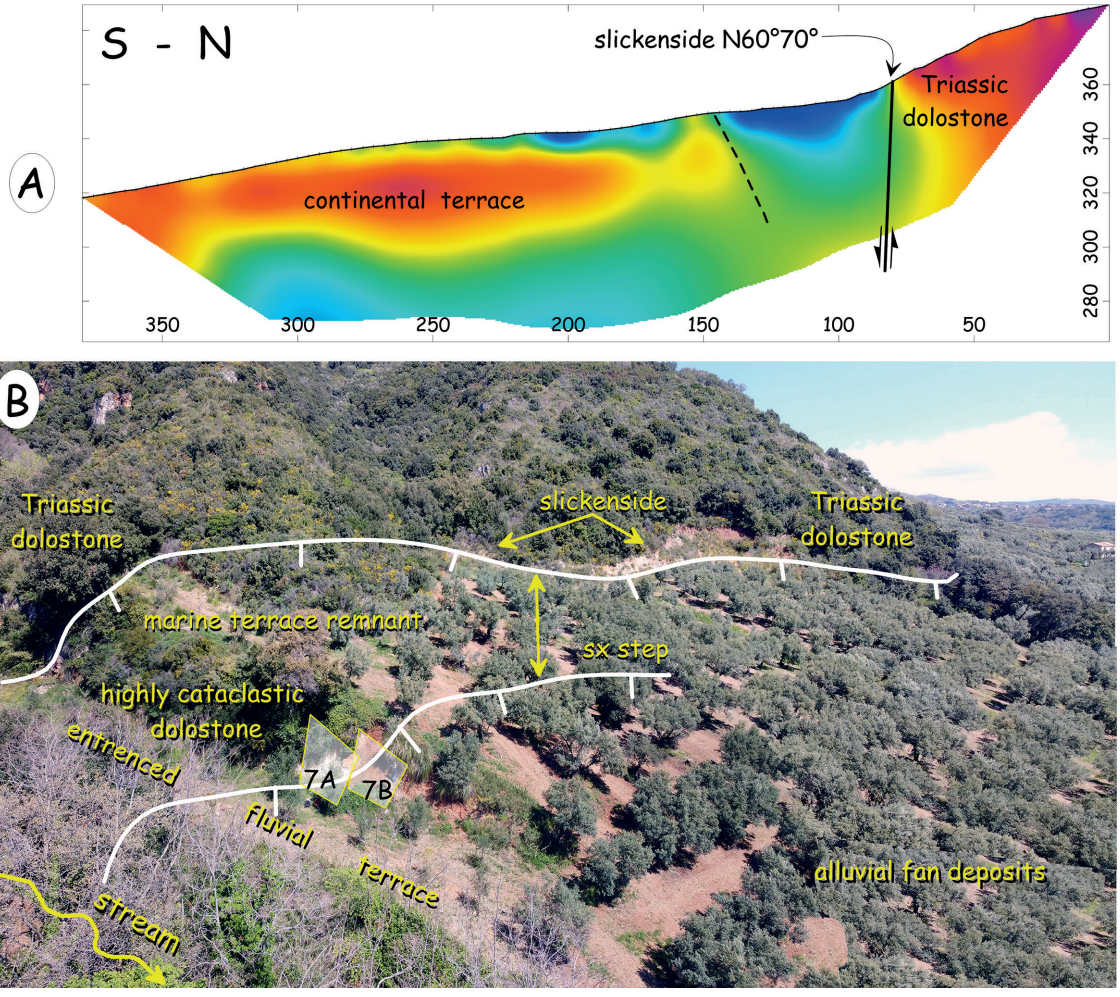

Fig. 6 - A) Pole-dipole electrical resistivity tomography conducted perpendicularly to the slickenside within the eastern border of the Caronte tectonic window; B) oblique aerial view looking NE at the site 2 (see Fig. 2). Two *en-echelon* splays of the Sant'Eufemia Fault displace the Triassic dolostone against the Middle Pleistocene marine terrace and the overlying recent alluvial fan deposits. Panels 7A and 7B correspond to the fault outcrops shown in Fig. 7.

resulting in the local formation of an alluvial fan over the hanging wall top surface. This fan was later incised and terraced by continued stream downcutting (Fig. 6B).

The fault zone was exposed by clearing dense, seasonal vegetation that had obscured all the valley flank, between the upper surface of the alluvial fan and the top of a younger terrace entrenched 6 m below. The outcrop consists of two sub-parallel exposures, located 3-4 m apart (7A and 7B in Fig. 6) and separated by a small oblique gully that has removed part of the footwall and the relative slickenside.

The excavation exposed a N80°striking, 83° dipping bedrock fault plane (5 in Fig. 7A), along which cemented marine sands and gravels were dragged and vertically displaced along the slickenside, forming a 10–20-centimetre-thick fault gouge (4 in Figs. 7A and 7B). These marine gravels are also faulted against reddish sandy deposits that extensively outcrop at the base of the hillslope (3 in Figs. 7A and 7B). A second sub-parallel excavation, located 3–4 m further back from the first, exposed the fault contact just beneath the fossilised top surface of the fan. Here, the fault separates fine, stratified fluvial gravels in a sandy matrix (2 in Fig. 7B) from coarse, reddish sandy deposits with scattered carbonate clasts, interpreted as eluvial-colluvial reworking of the alluvial fan deposits that mantle the terrace at the base of the hillslope (3 in Fig. 7B). The active soil layer (1 in Fig. 7B) includes a basal anthropogenic horizon composed of sub-rounded carbonate clasts embedded in a dark, organic-rich matrix. It lays over an erosional surface which is clearly offset of at least 0.5 m at the fault intersection, resulting in a thickening of pedogenic unit 1 on the hanging wall side (Fig. 7B). This displacement also affects the basal anthropogenic layer whose clasts appear to be dragged along the fault plane.

It is worth noting that the erosional surface corresponds to a reddish hardground with slightly cemented clasts, possibly representing the original top surface of the fossil alluvial fan prior to the onset of planting and intensive olive cultivation. Actually, such agricultural transformation was made possible in this area by the introduction of new farming techniques by the Benedictine

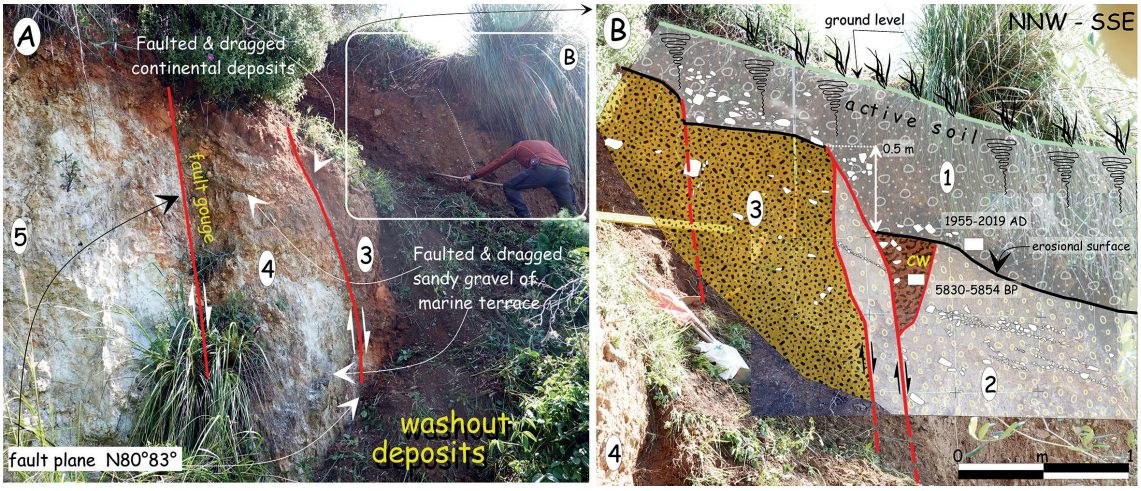

Fig. 7 - A) Close-up view of the fault zone between the Triassic dolostone (5) and the coarse sands of the marine terrace (4), separated by a fault-gauge made at the expense of the latter. In the background, the rounded rectangle indicates the outcrop area shown in panel B; B) palaeoseismological log of the continental succession where fine, stratified fluvial gravel (2) are faulted against reddish coarse sand with sparse carbonate clasts of alluvial origin (3). The erosional surface truncating units 2-3 is vertically offset by at least 0.5 m, producing a thickening of the above active soil level in the hanging-wall. Although the dated organic material is recent, the last faulting event is surely recent as well. On the other hand, the faulted colluvial wedge provided a middle Holocene age for a previous event.

monks of the nearby Abbey of Sant'Eufemia, owner of these lands, at the beginning in the 12th century (Donato, 2023).

In the hanging wall, beneath unit 1, a triangular CW is truncated at the top by the erosional surface and faulted against the fine fluvial gravels of unit 2. Notably, all stratigraphic units are faulted, with the likely exception of the upper portion of the organic soil, which appears to have been significantly reworked by agricultural activity related to modern intense olive cultivation.

Preliminary radiocarbon (^{14}C) dating of two samples (Table 1) indicates Holocene surface faulting. In particular, the most recent event produced displacement of the entire stratigraphic succession, even of the erosional surface at the base of the active soil. Although the material sampled at the bottom of the soil is extremely recent – implying that the entire unit may behave as a geochemically open system – the ultimate faulting event occurred within a stratigraphic context identical to the present one, indicating a very young age, potentially as recent as the 1638 earthquake. Evidence for earlier faulting events is provided by the formation and subsequent displacement of the CW. One of these events can be confidently dated to the early 6th millennium B.P. (^{14}C age of the CW), while the others predate the 1638 event, although their age remains undetermined.

6. Discussion and conclusions

The Lamezia-Catanzaro fault system is part of a left-lateral shear zone that entirely characterises the Catanzaro Through, a region of very high seismic hazard, hosting powerful, but still poorly known, seismogenic structures. This fault system is composed by south-dipping *en echelon* segments that were active during the Miocene, before shifting to right-lateral motion in the Pliocene-Early Pleistocene. While its current activity and seismogenic potential have been suggested by several authors, supporting geological, geomorphological, and geophysical evidence remains limited and inconclusive.

Nonetheless, for the first time we have provided reliable palaeoseismological evidence for the activity of the westernmost sector of the Lamezia-Catanzaro fault system, specifically of its ENE-WSW trending Sant'Eufemia normal fault. This fault aligns with the extensional regional regime inferred both from the few focal mechanisms of nearby $M_w > 4$ earthquakes, characterised by a NW–SE-trending T axis (Fig. 1), and recent Global Navigation Satellite System (GNSS)-based strain rate analyses in central Calabria (Palano *et al*., 2023), which also indicate a local ~NW-SE extension at approximately 0.7 mm/yr (Fig. 2). Despite this consistency, this fault exhibits a faint and elusive morphological expression, except where it crosses the Triassic dolostone within the Caronte tectonic window (dol in Fig. 2). In this area, at the base of the fault scarp, a younger splay striking N70°E and marked by a prominent slickenside indicates a rejuvenation of the main fault, which appears sealed upslope by ~Middle Pleistocene marine sandstone. Structural data taken along the carbonate slickenside yield a pseudo-focal mechanism consistent with normal fault, accompanied by a minor dextral component, with a T axis oriented N163° (Fig. 2).

The evidence collected at two separate sites – one in the Caronte tectonic window and the other above Nicastro town, in the metamorphic basement of the Sila plateau – indicates repeated surface faulting in both locations during the Holocene (sites 1 and 2 in Fig. 2).

Regarding the timing of the palaeo-earthquakes identified at both palaeoseismological sites, the oldest visible event occurred at the beginning of the 6th millennium B.P., as testified by the ^{14}C age of the CW at site 2. Other successive events have also been identified, although their ages are not yet adequately constrained by the data available. In contrast, the penultimate event

is robustly constrained in our investigation at around 700 A.D. (site 1), while the more recent event took place during the past millennium, with the 28 March 1638 earthquake (I_0 11, M_w 6.6) emerging as the only plausible and strongest historical candidate correlating with the evidence observed in both sites 1 and 2.

Regarding these two most recent events, it is intriguing to note that recent archaeological excavations at the Church of the Forty Martyrs, located near the Caronte tectonic window (~ site 2 in Fig. 2), revealed that the original 6th–7th century church was indeed destroyed around the 7th–8th century (Donato, 2015). The church was, then, rebuilt at least by the 10th century, and again destroyed and downsized in the 17th century. Curiously, some burials inside the church also date to around 600–700 A.D. and others to ~1600 A.D. [^{14}C age, in Donato (2015)].

As a concluding remark, considering that the 8 June event of the 1638 seismic sequence was generated by the Lakes Fault (inner Sila plateau), we observe that even the age of the medieval event along the Sant'Eufemia Fault closely aligns with the penultimate palaeo-earthquake identified on the Lakes Fault [7th century A.D.; Galli (2025)]. In other words, both faults, despite being 30–50 km apart, appear to have ruptured in close succession during two distinct time spans: one around 700 A.D. and another in 1638.

If this chain of events were true, the approximate recurrence interval for large earthquakes along these faults in historical times would be around 1,000 years, a timespan consistent with the return period estimated from the Middle Holocene for the Lakes Fault in five palaeoseismological trenches [i.e. ~1.2 kyr; Galli *et al*. (2007)]. It is evident, however, that the seismogenic source capable of generating such strong earthquakes must be longer than the ~14 km currently mapped for the onshore segment of the Sant'Eufemia Fault. Future field investigations will be essential to identify additional palaeoseismological key sites that can further refine the seismic history of this fault system. In parallel, ongoing and future geophysical studies of the tectonic setting in the Gulf of Sant'Eufemia (e.g. Corradino *et al*., 2021; Martorelli *et al*., 2023) may help delineate the possible offshore continuation of the 1638 rupture source.

Acknowledgments. We are grateful to P. Vasta for providing important field data and M. Palano for sharing his GNSS data. We thank E. Donato for the archaeological indications concerning the Church of the Forty Martyrs. The insightful observations of two anonymous reviewers strongly enhanced the original manuscript. The view and conclusion contained in this paper are those of the authors and should not be interpreted as necessarily representing the official policies, either expressed or implied, of the Italian Government.

REFERENCES

Allmendinger R.W., Cardozo N. and Fisher D.; 2012: *Structural geology algorithms: vectors and tensors*. University Press, Cambridge, UK, 302 pp.

Alvarez W.; 2005: *Structure of the Monte Reventino greenschist folds: a contribution to untangling the tectonic-transport history of Calabria, a key element in Italian tectonics*. J. Struct. Geol., 27, 1355-1378, doi: 10.1016/j.jsg.2005.05.012.

Amodio-Morelli L., Bonardi G., Colonna V., Dietrich D., Giunta G., Ippolito F., Liguori V., Lorenzoni S., Paglionico A., Perrone V., Piccarreta G., Russo M., Scandone P., Zanettin-Lorenzoni E. and Zuppetta A.; 1976: *L'arco Calabro-Peloritano nell'Orogene Appenninico Maghrebide (The Calabrian-Peloritan Arc in the Apennine-Maghrebide Orogen)*. Mem. Soc. Geol. Ital., 17, 1-60.

Anderson E.M.; 1951: *The dynamics of faulting and dyke formation with application to Britain.* Oliver and Boyed, Edinburgh, UK, 206 pp.

Angelier J.; 1990: *Inversion of field data in fault tectonics to obtain the regional stress. A new rapid direct inversion method by analytical means*. Geophys. J. Int., 103, 363-376.

Angelier J. and Mechler P.; 1977: *Sur une methode graphique de recherche des contraintes principales egalement utilisables en Tectonique et en Seismologie: la methode des diedres droits*. Bull. Soc. Geol. Fr., S7, 1309-1318, doi: 10.2113/gssgfbull.S7-XIX.6.1309.

Antronico L., Tansi C., Sorriso-Valvo M. and Gullà G.; 2001: *Carta litologico-strutturale e dei movimenti in massa della Stretta di Catanzaro (scala 1:50000)*. Consiglio Nazionale delle Ricerche - Gruppo Nazionale per la Difesa dalle Catastrofi Idrogeologiche, linea 2, S.EL.CA., Firenze, Italy, <www.cnr.it/prodotto/i/306512>.

Bonardi G., Cavazza W., Perrone V. and Rossi S.; 2001: *Calabria-Peloritani terrane and northern Ionian Sea*. In: Martini L.P. and Vai G.B. (eds), Anatomy of an orogen: the Apennines and adjacent Mediterranean basins, Kluwer Academic Publication, Dordrecht, The Nethertlands, pp. 287-306.

Brandt S. and Schenk V.; 2021: *Metamorphic response to Alpine thrusting of a crustal-scale basement nappe in southern Calabria (Italy).* J. Petrol., 61, 11-12, doi: 10.1093/petrology/egaa063.

Brutto F., Muto F., Loreto M.F., De Paola N., Tripodi V., Critelli S. and Facchin L.; 2016: *The Neogene-Quaternary geodynamic evolution of the central Calabrian Arc: a case study from the western Catanzaro Trough basin*. J. Geodyn., 102, 95-114, doi: 10.1016/j.jog.2016.09.002.

Brutto F., Muto F., Loreto M.F., D'Amico S., De Paola N., Tripodi V. and Critelli S.; 2018: *Quaternary stress field and faulting in the western part of the Catanzaro Trough (Calabria, southern Italy)*. In: D'Amico S. (ed), Moment tensor solutions, Springer Natural Hazards, Berlin, Germany, pp. 619-642, doi: 10.1007/978-3-319-77359-9_28.

Camassi R. and Stucchi M. (eds); 1997: *Un catalogo parametrico di terremoti di area italiana al di sopra della soglia di danno (vers. 4.1.1)*. Gruppo Nazionale per la Difesa dai Terremoti, Milano, Italy, 93 pp.

Cavazza W. and Decelles P.G.; 1998: *Upper Messinian siliciclastic rocks in southeastern Calabria (S Italy): paleotectonic and eustatic implications for the evolution of the central Mediterranean region*. Tectonophys., 298, 223-241, doi: 10.1016/S0040-1951(98)00186-3.

Chiarella D., Moretti M., Longhitano S. and Muto F.; 2016: *Deformed cross-stratified deposits in the Early Pleistocene tidally-dominated Catanzaro strait-fill succession, Calabrian Arc southern Italy: triggering mechanisms and environmental significance*. Sediment. Geol., 344, 277-289, doi: 10.1016/j.sedgeo.2016.05.003.

Corradino M., Pepe F., Burrato P., Kanari M., Parrino N., Bertotti G., Bosman A., Casalbore D., Ferranti L., Martorelli E., Monaco C., Sacchi M. and Tibor G.; 2021: *An integrated multiscale method for the Characterisation of Active Faults in Offshore Areas. The Case of Sant'Eufemia Gulf (Offshore Calabria, Italy)*. Front. Earth Sci., 9, doi: 10.3389/feart.2021.670557.

Critelli S., Muto F., Tripodi V. and Perri F.; 2013: *Link between thrust tectonics and sedimentation processes of stratigraphic sequences from the southern Apennines foreland basin system*, *Italy.* Rend. Soc. Geol. Ital., 25, 21-42, doi: 10.3301/ROL.2013.03.

Donato E.; 2015: *Sulle tracce del monastero bizantino dei Ss. Quaranta Martiri nel territorio di Lamezia Terme (Cz).* Quaderni di Archeologia, 5, 111-135.

Donato E.; 2023: *L'abbazia di Santa Eufemia e il suo territorio*. *Ricerche di Archeologia Medievale nella piana lametina*. Rubbettino Ed., Soveria Mannelli (CZ), Italy, 210 pp.

Faccenna C., Civetta L., D'Antonio M., Funiciello F., Margheriti L. and Piromallo C.; 2005: *Constraints on mantle circulation around the deforming Calabrian slab*. Geophys. Res. Lett., 32, L06311, doi: 10.1029/2004gl021874.

Galli P.; 2024: *Nearly simultaneous pairs and triplets of historical destructive earthquakes with distant epicenters in the Italian Apennines*. Seismol. Res. Lett., 95, 1057-1065, doi: 10.1785/0220230135.

Galli P.; 2025: *Lakes Fault, Italy*. In: Cinti F., Pantosti D., Schwartz D. and Klinger Y. (eds), The science and art of paleoseismology. Images of paleoearthquakes records from around the World, ISBN 979-12-80282-09-5, 116-119.

Galli P. and Bosi V.; 2003: *Catastrophic 1638 earthquakes in Calabria (southern Italy): new insight from paleoseismological investigation*. J. Geophys. Res., Solid Earth, 108, 1-20, doi: 10.1029/2001JB001713.

Galli P. and Scionti V.; 2006: *Two unknown M>6 historical earthquakes revealed by paleoseismological and archival researches in eastern Calabria (southern Italy). Seismotectonic implication*. Terra Nova, 18, 44-49, doi: 10.1111/j.1365-3121.2005.00658.x.

Galli P., Scionti V. and Spina V.; 2007: *New paleoseismic data from the Lakes and Serre faults (Calabria, southern Italy). Seismotectonic implication*. Boll. Soc. Geol. Ital., 126, 347-364.

Galli P., Spina V., Ilardo I. and Naso G.; 2010: *Evidence of active tectonics in southern Italy: the Rossano Fault (Calabria)*. In: Guarnieri P. (ed), Recent progress on earthquake geology, Nova Scientific Publisher Inc., New York, NY, USA, pp. 49-78.

Galli P., Peronace E., Quadrio B. and Esposito G.; 2014: *Earthquake fingerprints along fault scarps: a case study of the Irpinia 1980 earthquake fault (southern Apennines)*. Geomorphol., 206, 97-106.

Ghisetti F.; 1979: *Evoluzione neotettonica dei principali sistemi di faglie della Calabria centrale*. Boll. SGI, 98, 387-430.

Ghisetti F. and Vezzani L.; 1982: *Different styles of deformation in the Calabrian Arc (southern Italy): implications for a seismotectonic zoning*. Tectonophys., 85, 149-165.

Guidoboni E., Ferrari G., Mariotti D., Comastri A., Tarabusi G., Sgattoni G. and Valensise G.; 2018: *CFTI5Med, Catalogo dei Forti Terremoti in Italia (461 a.C.-1997) e nell'area Mediterranea (760 a.C.-1500)*. Istituto Nazionale di Geofisica e Vulcanologia (INGV), doi: 10.6092/ingv.it-cfti5.

Kircher A.; 1665: *Mundus subterraneus in XII libros digestus*. Joannes Jansson and Elizeus Weyerstraet, Amsterdam, The Netherlands, 441 pp., doi: 10.26035/epfl-plume-1454.

Lavecchia G., Bello S., Andrenacci C., Cirillo D., Pietrolungo F., Talone D., Ferrarini F., de Nardis R., Galli P., Faure Walker J., Sgambato C., Menichetti M., Monaco C., Gambino S., De Guidi G., Barreca G., Carnemolla G., Brighenti F., Giuffrida S., Pirrotta C., Carboni F., Ferranti L., Valoroso L., Toscani G., Barchi M.R., Roberts G. and Brozzetti F.; 2024: *QUIN 2.0 - new release of the Quaternary fault strain indicators database from the southern Apennines of Italy.* Sci. Data, 11, doi: 10.1038/s41597-024-03008-6.

Longhitano S.G., Chiarella D. and Muto F.; 2014: *Three-dimensional to two-dimensional cross-strata transition in the lower Pleistocene Catanzaro tidal strait transgressive succession (southern Italy)*. Sedimentology, 61, 2136-2171, doi: 10.1111/sed.12138.

Loreto M.F., Fracassi U., Franzo A., Del Negro P., Zgur F. and Facchin L.; 2013: *Approaching the seismogenic source of the Calabria 8 September 1905 earthquake: new geophysical, geological and biochemical data from the S. Eufemia Gulf (S Italy).* Mar. Geol., 343, 62-75, doi: 10.1016/j.margeo.2013.06.016.

Loreto M.F., Capotondi L., Insinga D.D., Molisso F., Vigliotti L., Albertazzi S., Giordano P., Muto F. and Romano S.; 2023: *Slip-rates and time recurrences of the seismogenic Sant'Eufemia normal fault (SE Tyrrhenian Sea), a multiscale and multidisciplinary approach*. Mar. Pet. Geol., 156, 106453, doi: 10.1016/j.marpetgeo.2023.106453.

Malinverno A. and Ryan W.B.F.; 1986: *Extension in the Tyrrhenian Sea and shortening in the Apennines as result of arc migration driven by sinking of the lithosphere*. Tectonics, 5, 227-245, doi: 10.1029/TC005i002p00227.

Martorelli E., Casalbore D., Bosman A., Pepe F., Corradino M., de Nardis R., Monaco C. and Sposato A.; 2023: *Basin-scale interaction between post-LGM faulting and morpho-sedimentary processes in the S. Eufemia Gulf (southern Tyrrhenian Sea)*. Geomorphol., 436, doi: 10.1016/j.geomorph.2023.108775.

Moretti A.; 2000: *Il database delle faglie capaci della Calabria: stato attuale delle conoscenze*. In: Galadini F., Meletti C. and Rebez A. (eds), Le ricerche del GNDT nel campo della pericolosità sismica (1996-1999), CNR-Gruppo Nazionale per la Difesa dai Terremoti, ISBN88-900449-2-6, pp. 219-226.

Muto F. and Perri E.; 2002: *Tectonic-sedimentary evolution of the Amantea basin, western Calabria.* Boll. Soc. Geol. Ital., 121, 1-19.

Muto F., Spina V., Tripodi V., Critelli S. and Roda C.; 2014: *Neogene tectonostratigraphic evolution of allochthonous terranes in the eastern Calabrian foreland (southern Italy)*. Ital. J. Geosci., 133, 455-473.

Ogniben L.; 1969: *Schema introduttivo alla geologia del confine calabro-lucano (Introductory scheme to the geology of the Calabrian-Lucanian boundary)*. Mem. Soc. Geol. Ital., 8, 453-763.

Ortolano G., Visalli R., Fazio E., Fiannacca P., Godard G., Pezzino A., Punturo R., Sacco V. and Cirrincione R.; 2020: *Tectono-metamorphic evolution of the Calabria continental lower crust: the case of the Sila Piccola Massif*. Int. J. Earth Sci., 109, 1295-1319.

Palano M., Billi A., Conti A., Cuffaro M., Orecchio B., Presti D., Scolaro S., Sparacino F. and Totaro C.; 2023: *The intra-orogenic normal Lakes Fault (Sila, Calabria, southern Italy): new insights from geodetic and seismological data*. Ital. J. Geosci., 142, 384-397, doi: 10.3301/IJG.2023.18.

Piluso E., Cirrincione R. and Morten L.; 2000: *Ophiolite of the Calabrian Arc and their relationships with the crystalline basement (Catena Costiera and Sila Piccola, Calabria, southern Italy*). Ofiolite, 25, 117-140.

Pirrotta C., Barberi G., Barreca G., Brighenti F., Carnemolla F., De Guidi G., Monaco C., Pepe F. and Scarfì L.; 2021: *Recent activity and kinematics of the bounding faults of the Catanzaro Trough (central Calabria, Italy): new morphotectonic, geodetic and seismological data*. Geosci., 11, doi: 10.3390/geosciences11100405.

Pirrotta C., Parrino N., Pepe F., Tansi C. and Monaco C.; 2022: *Geomorphological and morphometric analyses of the Catanzaro Trough (central Calabrian Arc, southern Italy): seismotectonic implications*. Geosci., 12, 324, doi: 10.3390/geosciences12090324.

Postpischl D. (ed); 1985: *Catalogo dei terremoti italiani dall'anno 1000 al 1980*. CNR, Progetto Finalizzato Geodinamica, Sottoprogetto Rischio Sismico e Ingegneria Sismica, Quaderni de la Ricerca Scientifica, 114, 2B, Bologna, Italy, [riedizione in versione digitale a cura di: Peronace E., Galli P. and Gasperini P., CNR Edizioni, Roma, Italy, 2025, ISBN (ed. digitale) 978 978 88 8080 735 3].

Punzo M., Cianflone G., Cavuoto G., De Rosa R., Gallo P., Lirer F., Pelosi N. and Di Fiore V.; 2021: *Active and passive seismic methods to explore areas of active faulting. The case of Lamezia Terme (Calabria, southern Italy)*. J. Appl. Geophys., 188, 021, doi: 10.1016/j.jappgeo.2021.104316.

Rovida A., Locati M., Camassi R., Lolli B., Gasperini P. and Antonucci A. (eds); 2022: *Catalogo Parametrico dei Terremoti Italiani (CPTI15), versione 4.0*. Istituto Nazionale di Geofisica e Vulcanologia (INGV), Roma, Italy, doi: 10.13127/cpti/cpti15.4.

Ruello M.R., Cinque A., Di Donato V., Molisso F., Terrasi F. and Russo Ermolli E.; 2017: *Interplay between sea level rise and tectonics in the Holocene evolution of the St. Eufemia Plain (Calabria, Italy)*. J. Coast. Conserv., 21, 903-915, doi: 10.1007/s11852-017-0558-9.

Russo Ermolli E., Ruello M.R., Cicala L., Di Lorenzo H., Molisso F. and Pacciarelli M.; 2018: *An 8300-yr record of environmental and cultural changes in the Sant'Eufemia Plain (Calabria, Italy)*. Quat. Int., 483, 39-56, doi: 10.1016/j.quaint.2018.01.033.

Scionti V. and Galli P.; 2005: *Nuovi dati sulla sismicità della Calabria nei secoli del Viceregno*. Rogerius - Boll. Ist. Bibl. Cal., 8, 65-84.

Scionti V., Galli P. and Chiodo G.; 2006: *The Calabrian seismicity during the Viceroyalty of Naples: sources silence or silent sources? The case of the strong 1744 earthquake*. Boll. Geof. Teor. Appl., 47, 53-72.

Sieberg A.; 1930: *Geologie der Erdbeben*. Handb. Geophys., 2, 552-554.

Sorriso-Valvo M. and Tansi C.; 1996; *Carta delle grandi frane e delle deformazioni gravitative profonde di versante della Calabria*. Geogr. Fis. Dinam. Quat., 19, 395-408.

Tansi C., Muto F., Critelli S. and Iovine G.; 2007: *Neogene-Quaternary strike-slip tectonics in the central Calabria Arc (southern Italy)*. J. Geodyn., 43, 397-414, doi: 10.1016/j.jog.2006.10.006.

Tortorici L.; 1982: *Lineamenti geologico-strutturali dell'Arco Calabro Peloritano (Geologic-structural lineaments of the Calabrian-Peloritan Arc)*. Soc. Ital. Min. Pet., 38, 927-940.

Tortorici G., Bianca M., Monaco C., Tortorici L., Tansi C., De Guidi G. and Catalano S.; 2002: *Quaternary normal faulting and marine terracing in the area of Capo Vaticano and S. Eufemia plain (southern Calabria)*. Stud. Geol. Camerti, 1, 155-171.

Van Dijk J.P., Bello M., Brancaleoni G.P., Cantarella G., Costa V., Frixa A., Golfetto F., Merlini S., Riva M., Torricelli S., Toscano C. and Zerilli A.; 2000: *A regional structural model for the northern sector of the Calabrian Arc (southern Italy)*. Tectonophys., 324, 267-320, doi: 10.1016/S0040-1951(00)00139-6.

Corresponding author: Paolo Galli
Presidenza del Consiglio dei Ministri
Dipartimento della Protezione Civile, Servizio Rischio Sismico
Via Vitorchiano 4, 00189 Roma, Italy
Phone: +39 06 68204892, e-mail: paolo.galli@protezionecivile.it